P. Aryan, A. Kotousov, C.T. Ng and S. Wildy

Reconstruction of baseline time-trace under changing environmental and operational conditions

Smart Materials and Structures, 2016; 25(3):035018-1-035018-10

Reconstruction of base-line time-trace under changing environmental and operational conditions

P Aryan[1], A Kotousov[1], C T Ng[2]and S Wildy[3]

[1]School of Mechanical Engineering, University of Adelaide, Adelaide, Australia
[2]School of Civil, Environmental & Mining Engineering, University of Adelaide, Adelaide, Australia
[3]School of Computer Science, Engineering and Mathematics, Flinders University, Adelaide, Australia
E-mail: pouria.aryan@adelaide.edu.eu

Keywords: Damage detection, guided waves, temperature compensation, changing EOC, 3D laser vibrometry, base-line time-trace.

Abstract. Compensation of changing environmental and operational conditions (EOC) is often necessary when using guided-wave based techniques for structural health monitoring in real-world applications. Many studies have demonstrated that the effect of changing EOC can mask damage to a degree that a critical defect might not be detected. Several effective strategies, specifically for compensating the temperature variations, have been developed in recent years. However, many other factors, such as changing humidity and boundary conditions or degradation of material properties, have not received much attention. This paper describes a practical method for reconstruction of the base-line time-trace corresponding to the current EOC. Thus, there is no need for differentiation or compensation procedures when using this method for damage diagnosis. It is based on 3D surface measurements of the velocity field near the actuator using laser vibrometry, in conjunction with high-fidelity finite element simulations of guided wave propagation in free from defects structure. To demonstrate the feasibility and efficiency of the proposed method we provide several examples of the reconstruction and damage detection.

1. Introduction

The detection of damage is often necessary for safe and efficient operation of current and future infrastructure. Historically damage has been detected by performing an inspection with sensors, which are placed temporarily on the surface of a structure and removed after all required measurements are conducted. This procedure is repeated if subsequent inspections are needed. Structural Health Monitoring (SHM) normally refers to a process, and sometimes extends to the equipment and instrumentation for in situ monitoring of the structural integrity and damage diagnosis using real-time data obtained from an embedded sensor network. Thus, there is no need for disassembly of components to be inspected as the sensors are permanently attached, becoming a part of the structure. This approach allows for a continuous and automated monitoring of critical structural components and is capable to provide a substantial reduction of the amount of time that the structure is out of operation. As a result, the importance of SHM to enhance the reliability and reduce the life-cycle costs is now widely recognised [1]. Current applications of SHM for damage detection include aircrafts, bridges, offshore wind power plants, pipes and rails.

In recent years significant progress was achieved in the development of SHM procedures based on guided waves [2]. Guided waves arise from interaction of normal and shear waves in bounded media with the boundaries. Lamb waves, which are the guided waves propagating in traction-free thin plates, are the most widely used for damage detection. The potential of using guided waves for Non-Destructive Testing (NDT) has been realised shortly after their existence was proven experimentally by Schoch in 1951. In 1961, Worlton was the first who utilised Lamb waves for damage detection. Over the past 20 years guided waves have found many applications in SHM driven by a step advance in fabrication technologies of piezo-electric transducers (PZTs). These new technologies have enabled the miniaturization of bulk ultrasonic sensors and actuators and a significant reduction of cost in mass production. Compared to different types of sensors utilised for in situ systems, such as strain or vibration gauges, which passively record data, piezo-electric devices can function as both actuator and sensor [3, 4].

Many studies in the past have demonstrated a very high sensitivity of guided waves have to various types of structural damage and their ability to propagate over large distances without significant decay. This offers the possibility of inspecting the entire cross-section of the beam, plate or shell component using a small number of sensors [5]. The fact that the entire thickness can be

interrogated makes it possible to detect hidden damage (e.g. embedded cracks [6-9] and delamination in composites [10-13]) as well as on the surface (e.g. corrosion or wear [14-16]).

Fundamental modes at relatively low frequencies are normally utilised in SHM, as at higher frequencies the presence of multiple modes makes the resulting signals extremely complex and difficult to analyse. The wavelength of the excited signal has to be smaller than characteristic dimensions of the targeted damage. Therefore, the fundamental anti-symmetric mode or flexural mode (A_o) is more preferable and more sensitive to damage as its wavelength is shorter at the same frequency than that of the symmetric mode (S_o). In particular, it was reported, that the A_o mode is very efficient for detecting delamination damage in composites and surface damage in isotropic plate and shell components [17, 18]. However, the A_o mode is highly dispersive and requires stringent conditions in experiments to prevent energy dissipation. In addition, FE simulations involving the A_o mode require a higher mesh density due to a substantial variation of stresses across the thickness, which significantly increases computational time. In contrast, the stress distribution across the thickness corresponding to the S_o mode is largely uniform, specifically at low frequencies, and it is preferable for damage detection of through-the-thickness defects, such as cracks and holes [2].

A typical guided wave SHM system comprises of a number of transducers permanently bonded to the surface of a structure. One of the transducers (acting as a transmitter) is excited with a tone burst of few cycles generating a guided stress wave that propagates along the structure. The time-domain response (time-traces) is then recorded by either the transmitter and/or other transducers. This process is repeated using different transducers as the transmitters. The majority of the guided waves damage detection techniques are based on the analysis of algebraic difference between the current time-trace and an initial base-line time-trace recorded for the structure. The signal remaining after the substruction of a base-line time-trace is referred to as a residual time trace. This residual time-trace can be related to the effect of damage provided that it is not affected by coherent noise or changing environmental and operational conditions (EOC).

The guided wave SHM system can usually operate in two modes: in a pulse-echo mode where damage is detected by examining waves reflected and/or scattered from the damage, or in a pitch-catch mode, when transmitted waves instead of reflected waves are analysed for the presence of damage. In both modes the damage detection is based on the following prerequisites [5]:

(i) base-line time-traces are available from the structure when in pristine condition,

(ii) the residual time-traces can be observed and related to damage and;

(iii) the threshold level of the residual time-trace, which indicates the presence of a critical damage, can also be established by utilising the available base-line time-traces.

The current limiting factor of SHM systems based on guided waves is the difficulty in differentiating the residual time-traces due to damage and those caused by changing EOC. SHM systems which have been developed in the last two decades in laboratory conditions can often fail in real-world situations. The influence of changing temperature, humidity, boundary conditions, degradation of material properties are all capable of masking damage to a degree that a critical defect might not be detected. A number of recent studies (e.g. Konstantinidis *et al.*[19] and Sohn *et al.* [20],) demonstrated that the signal attenuation and time of flight, which are commonly used as damage-sensitive indicators, are also highly sensitive to EOC. Hence, if the effect of EOC is disregarded in the development of guided wave damage detection algorithms, it could lead to false alarms and/or decreased damage sensitivity.

It has been reported in many articles [21-24] that the primary effect of temperature is stretching or compressing the signal recorded from the structure, and a secondary effect is a distortion of the shape. For small temperature variations of a few degrees, the effect of temperature changes on transducer performance is significantly less than on wave propagation. In this case, stretching or compressing occurs due to modification of the wave propagation properties of the material with temperature (wave speeds), while the change in the shape is mainly a results of the modifications of the parameters of the acoustical absorption (wave attenuation). For large temperature changes, the variation of the transducer and bonding properties become more significant [25]. Several experimental studies [23, 26, 27] have reported that the time of flight and the amplitude normally increase with temperature. Thus, in recent years a great effort has been made to compensate the temperature effects. Two common temperature compensation methods are briefly discussed in the proceeding paragraph.

Lu and Michaels [26] suggested a temperature compensation method called Base-line Signal Stretch (BSS) in which the actual time-trace is transformed by a time dilation or compression to match the selected base-line time trace. If the algebraic subtraction between the transformed time-trace and a base-line time-trace exceeded a threshold, then damage was detected. The BSS method needs only one base-line trace, but it is limited in the range of temperature changes that can be accommodated. Dan *et al.* [28] noted that the applicability of this method to complex structures may represent a challenging endeavour due to boundary reflections and that the rate of change of

the wave speed is frequency dependent. This can be important in the context of using of wave-packets as base-line time-traces. In contrast, an Optimal Base-line Subtraction (OBS) method utilises time-traces recorded from the pristine structure at discreet temperatures [29]. A least-squares error approach is then used to select the most appropriate base-line time-trace to evaluate the residual time trace. Both temperature compensation methods normally perform well, however these methods cannot be generalised or applied when, in addition to temperature, there are other changing EOC that affect the base-line time-trace. For example, these methods have difficulty in differentiating between a progressive failure of PZT bonding and progressive damage to the structure. Moreover, the influence of different EOC could have a synergistic effect leading to producing false alarms.

This paper describes a practical method for reconstruction of the base-line time-trace for a free from defect structure corresponding to the actual structural, operating, and environmental conditions. In particular, with this method it is possible to detect structural damage in the presence of unknown and unmeasured temperature variations. Thus, there is no need for differentiation or compensation procedures when using this method for damage detection. It utilises 3D Scanning Laser Vibrometry (SLV) and transient high-fidelity Finite Element (FE) simulations of guided wave propagation. The conceptual idea of this method is based on a physical recording of the actual 3D velocity/displacement fields around the PZT (scanning area) and prescribing these fields to the corresponding finite element model representing the free-from-defect structure. The scanning area encapsulates the PZT avoiding the necessity to model the PZT response, which is often extremely complex and can be severely affected by EOC as discussed earlier. The materials data, which is needed for the numerical simulations, is extracted from the analysis of the wave propagation in the scanning area. Therefore, the method can compensate progressive changes of material properties of the inspected component with time. The paper demonstrates the feasibility of the reconstruction of the base-line time-trace describes a practical application of the developed method to damage detection in the case of changing temperature.

It is recognised that the use of SLV or other 3D non-contact measurement systems, as well as high-fidelity transient FE simulations, can significantly increase the cost of damage diagnostics. However, with the advance of computational power, numerical approaches and laser technologies, this cost will eventually decrease exponentially with time. Moreover, this method can be useful for damage inspections of hard-to-reach locations, or for the generation of periodical updates of the base-line time-traces in the case of changing of various EOC.

This paper initially introduces the concept of the proposed new method for the reconstruction of the base-line time-trace. This is followed by the results and discussion of the experimental and numerical studies conducted to demonstrate the practical reconstruction of the base-line signal for isotropic plates, as well as detection of damage in the case of changing temperature. Finally, a conclusion is presented, summarising the future work.

2. The Method

The concept of the proposed method can be explained with a help of two spaces: the physical space and modelling space, as illustrated in figure 1. The physical space represents the actual plate or shell component to be inspected, which is equipped with a PZT generating a burst signal of certain wavelength, λ, (frequency). The measurement system incorporates a 3D Scanning Laser Vibrometer (SLV), which records the resultant transient velocity/displacement at various points located in the scanning area, illustrated in figure 1. The time-trace at a remote measurement location (P), which also can be collected with traditional PZT, is then utilised for damage diagnostics of the component. The surface displacement over the scanning area, which encapsulates PZT, and at a remote location, P, are recorded and utilised in the modelling space for the reconstruction of the baseline time-trace and defect signature analysis, respectively. The main feature of the proposed method is that the base-line time-trace in this method is obtained or reconstructed using a modelling approach.

The modelling space, seen in figure 1, represents an accurate Finite Element (FE) model of the structural component excluding a cylindrical volume (dummy volume) with the PZT attached to its free surface. The transient displacements as recorded over the scanning area of the actual structure are prescribed to the corresponding nodes of the FE mesh. Our modelling results indicate that for thin plates the dummy volume does not affect the time-traces at remote locations if the thickness of the area with prescribed boundary conditions is larger than approximately half of wavelength of the generated signal. Thus, this volume as well as a PZT response can be simply ignored in the numerical reconstruction of the base-line time-trace. Therefore, there is no need to analyse a very complicated interaction between the PZT, bonding and the structure, which can be severely affected by EOC. Nevertheless, the effect of EOC on material properties of the structure cannot be compensated with the proposed method and it needs special consideration.

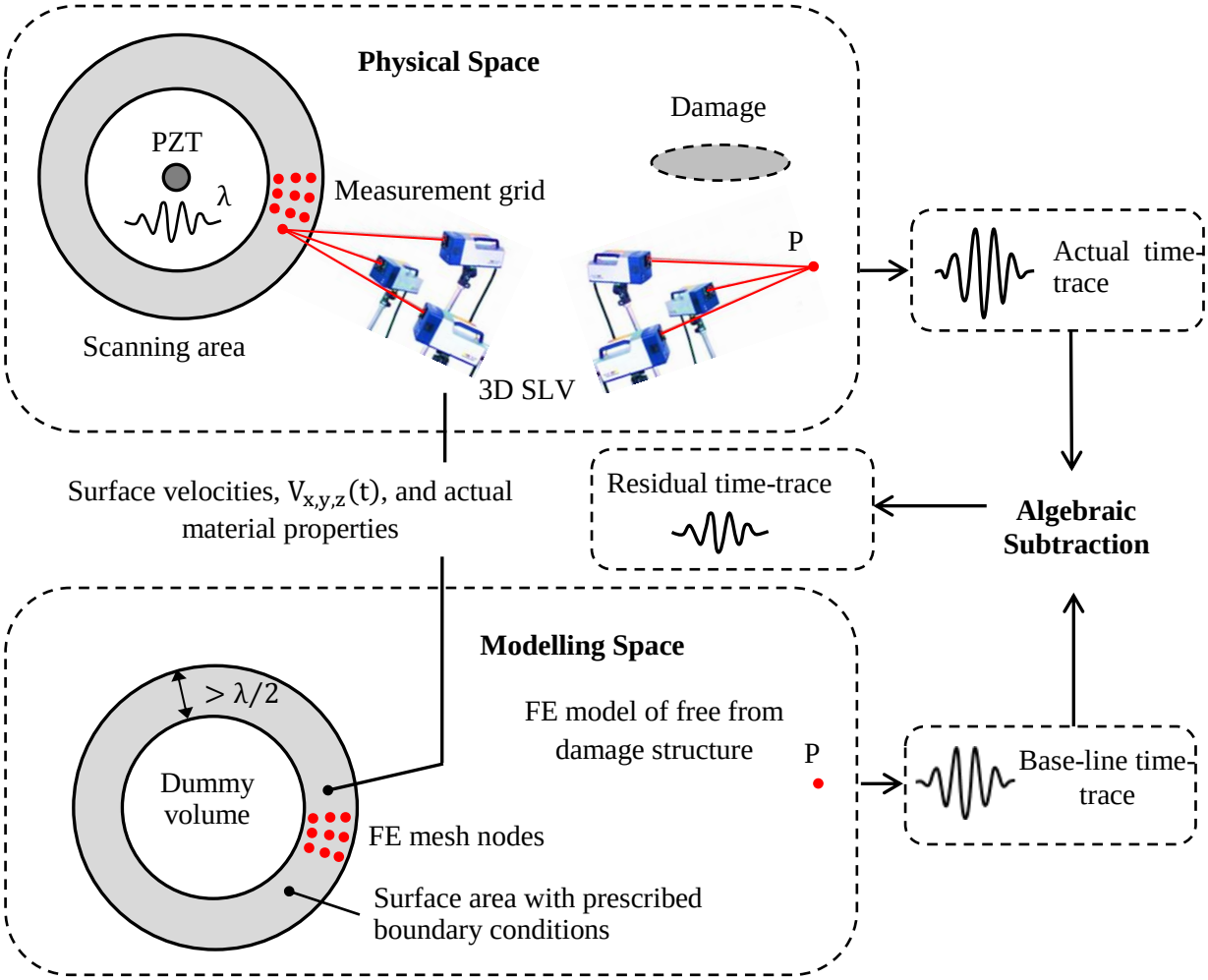

Figure 1: Concept of the proposed method illustrating the damage diagnostics in thin-walled structural components.

For the numerical reconstruction of the base-line time-trace the actual material properties corresponding to the current EOC can be identified from the wave propagation inside the scanning area. There are several well-known techniques for recovery of material properties, for example, from the measured phase velocity dispersion relations for both anisotropic and isotropic materials. For isotropic plate, the experimental data can be curve fitted to the theoretical equation [30]:

$$C_{ph}(f) = \left[\frac{\rho}{E}\frac{\rho}{\mu}(1-\nu^2) - \frac{\rho}{E}\frac{12}{h^2}(1-\nu^2)\frac{1}{2\pi f^2}\right] \qquad (1)$$

where C_{ph} is the phase velocity, f is the central frequency, ρ is the density of the material, h is the plate thickness, E is Young's modulus, μ is shear modulus and ν is Poisson's ratio.

The phase velocity, which is the ratio of the angular velocity, ω, and wave number, k, or

$$C_{ph}(f) = \frac{\omega}{k} = \frac{2\pi f}{k(f)} \tag{2}$$

can be determined from the phase spectra of time-dependent signals, measured at points along the radial lines, which starts from the excitation source (PZT). If $\Delta r = (r_2 - r_1)$ is the distance between such two points, and $\Delta\phi(f)$ is the phase difference as a function of a frequency, f, determined from the Fourier transformed signal, then the wave number $k(f)$ and the phase velocity can be calculated as

$$k(f) = -\frac{\Delta\phi}{\Delta r} \tag{3}$$

and

$$C_{ph}(f) = -\frac{2\pi f \Delta r}{\Delta\phi} \tag{4}$$

In order to avoid $\pm 2n\pi$ uncertainties, several measurement points along the radial line can be taken, so the value of n can be identified. The measuring points have to be selected in the way that the approximation of the centrally induced flexural waves by plane waves is reasonably accurate and that the input signal has passed the measuring point before the first reflection arrives.

Once the phase velocity, $C_{ph}(f)$, is determined , using least square optimisation and, for example, E/ρ as the parameter to be fit the actual value of this ratio can be identified, provided all other parameters, such as thickness and Poisson's ratio are known. An application of this technique to the identification of the ratio E/ρ an aluminium alloy plate, which was used in experimental studies (Section 3), is shown in figure 2. Here, the phase velocity was measured for 3 mm thickness aluminium plate subjected to A_o mode excitation. Assuming Poisson's ratio, ν = 0.3, (in general, changing Poisson's ratio does not significantly affect the optimisation result) $E/\rho = 27.2$ and 25.6 MN/kg were obtained for room temperature of 20^{o}C and elevated temperature of 60^{o}C, respectively. The effect of temperature expansion on the plate thickness is small and can be disregarded.

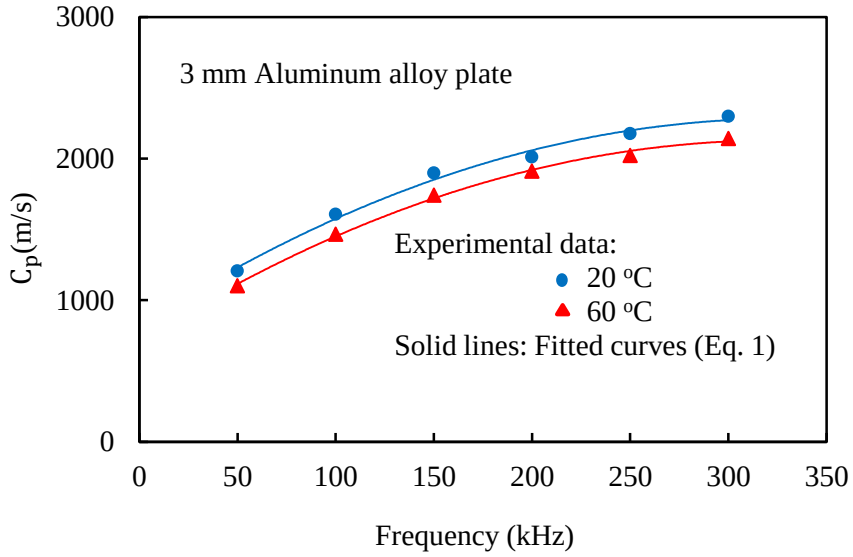

Figure 2: Phase velocity measurements (points) and the fitted curve for the 3 mm thickness aluminium plate at room and elevated temperatures.

If several parameters are unknown then a multi-parametric optimisation can be conducted in order to recover the actual material parameters of the structure. It is clear that the size and the shape of the scanning area have to be adequate for the determination of the phase velocity and recovery of the material properties, specifically for composite materials. However, these issues are beyond the scope of the current paper and were previously investigated in a number of articles for both isotropic and anisotropic materials [31-35].

3. Practical Implementation

This section presents practical implementations of the proposed method to the reconstruction of the base-line time-trace and damage detection in isotropic plates. In the beginning we will describe the experimental rig. Further, we briefly outline the numerical approach as the details of the FE model and simulations have been described elsewhere. Then, we will demonstrate the reconstruction of the base-line time-trace under changing temperature conditions with the proposed method. Finally, we will apply this method for damage detection with a simple SHM system operating in the pitch-catch mode.

3.1 Experimental Rig

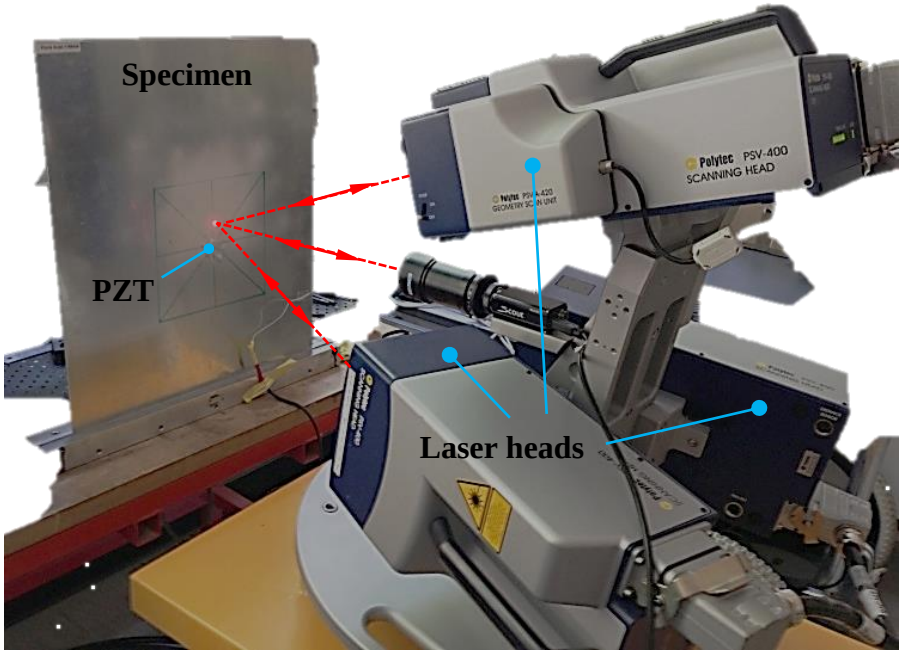

Figure 3: Picture of the experimental rig showing the 3 laser heads of the SLV for the 3mm thickness aluminium plate.

A picture of the experimental rig is shown in figure 3. The test specimen represents a 3 mm thick aluminium alloy plate with a size 500 mm by 500 mm aluminium plate allowing large propagation distances. For Lamb wave generation, a disk-shaped PZT piezoceramic made of PZ 27 with 10 mm in diametre and 3 mm in thickness dimensions with a backing mass of the same size made of brass was glued on the surface in the middle of the plates. Five cycle tune-bursts modulated by Hanning

window with central frequencies between 100 to 300 kHz were used in the experiments. As expected, the wave propagation was dominated by anti-symmetric A_o mode. These tune-bursts were generated by the SLV's in-built function generator and amplified before being transmitted to the PZT. The signal excitation was repeated and recorded 200 times for each excitation frequency and at every measurement point, averaged and filtered to improve the signal-to-noise ratio (SNR). The interval between excitations was approximately 9 ms, which was sufficient to avoid the interference between the consequently generated signals. The data recording and signal generation stages were synchronized and controlled by the SLV computer.

3.2 Laser Scanning and Signal Conditioning

The 3D SLV includes three laser heads each consists of a vibrometer sensor that are connected to a controller and a digital camera. A junction box as an interface between the sensor heads, the controller and the data acquisition system. The velocity decoder resolves the changes in frequency due to the Doppler shift to a voltage proportional to the measured velocity. Each scanning head can measure the velocity along its laser line so the velocity of one measurement point is obtained at three different angels as shown in figure 3.The 3D velocity in Cartesian coordinate system is then obtained based on an orthogonal decomposition. The laser heads must be properly aligned. More specific details regarding 2D and 3D alignment can be found in [36].

The PSV-400 SLV with a sampling frequency of 2.5 MHz was used to measure and record 3D velocity points over the scanning area, see figure 1, and at remote locations. With laser vibrometry the best SNR would be normally obtained for a highly polished surface. However, it only occurs for near-normal scanning angles, which are unachievable with 3D scanning laser systems, which measure velocities using the Doppler Effect at substantially different angles in order to resolve the measured velocities in three orthogonal components. Opposite to a polished surface, a rough or painted surface provides a more spatially uniform diffusive optical backscatter field; therefore, the SNR is more consistent over the scanned surface. In the current work we used Ardrox spray, which was applied to the surface of the aluminium plate, to achieve better SNR.

To simplify the prescription of boundary conditions for the numerical reconstruction of the base-line time-trace the measurement grid size was selected to be exactly the same as in the numerical simulations with the characteristic size approximately 10 smaller than the wavelength of the generated A_o mode. The measured signal was 200 times averaged at each measurement point to

improve the SNR. A band pass filter was implemented by multiplying the frequency spectra of the velocity time-traces obtained using the Fourier transform with a Gaussian window centred at the excitation frequency and with a bandwidth of 100 kHz. Once the frequency spectra have been filtered, they were transformed back into the time domain. The obtained velocity field at the grid and measurement points was integrated over time to provide the corresponding displacement components obtained by the software.

3.3 Reconstruction of Base-Line Time-Trace

Figure 4 shows a schematic drawing of the experimental arrangement. Two measurements points, P_1 and P_2 were located at a distance of 100 mm from the PZT equipped with a backing mass. The scanning area represents two rings on the both sides of the plate of 5 mm width and 50 mm radius. A cylindrical blind hole with a radius of 5 mm and depth 1.5 mm were milled at a distance of 75 mm from the PZT simulating structural damage. The time-trace at point P_1 was used to compare the actual base-line time-trace with the reconstructed from the numerical simulations. The residual time trace at point P_2 was used for damage detection. The separation between the blind hole and P_1 (175 mm) was sufficient to avoid the effect of the blind hole and free plate boundaries on the base-line time-trace recorded at P_1.

An elevated and ambient (room) temperature was considered. The required heating was introduced by a heat gun, which was directed to the middle of the plate. Temperature was monitored in three discreet points, near the centre of the plate and the measurement points P_1 and P_2. The temperature was assumed constant over the measured path and during wave propagation.

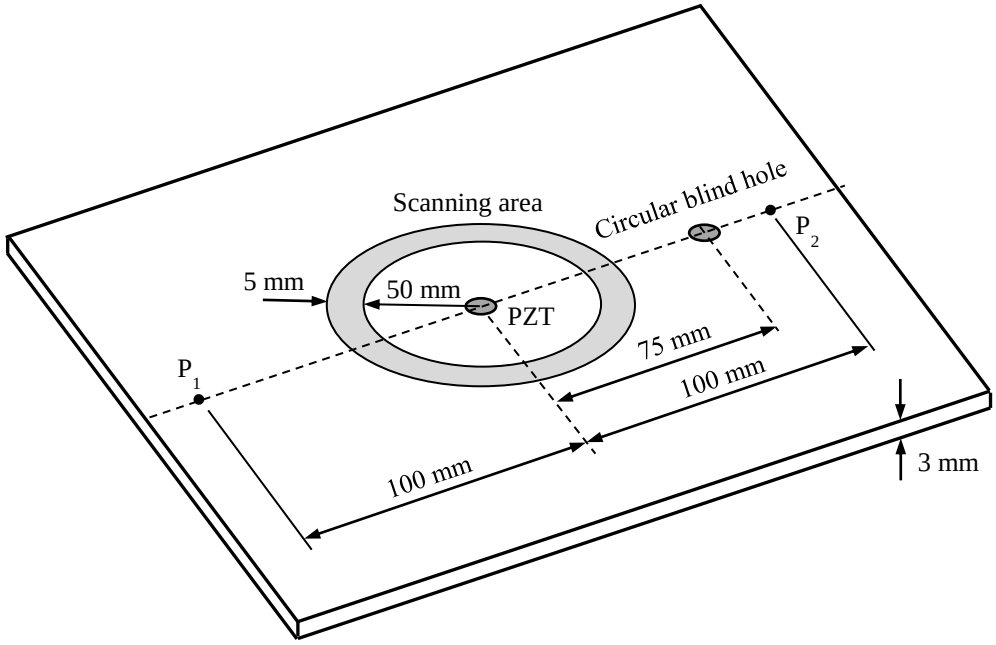

Figure 4: Experimental implementation of the proposed method for an isotropic plate with damage (blind hole)

Base-line time traces were collected for a set of equally spaced frequencies, covering a bandwidth of 100 – 300 kHz over two sets of temperature ranges. Figure 5 shows an example of the effect of the time-trace of the normalised out-of-plane displacements U_z at point P_1 at different temperatures (20^oC and 60^oC) for 200 kHz excitation central frequency.

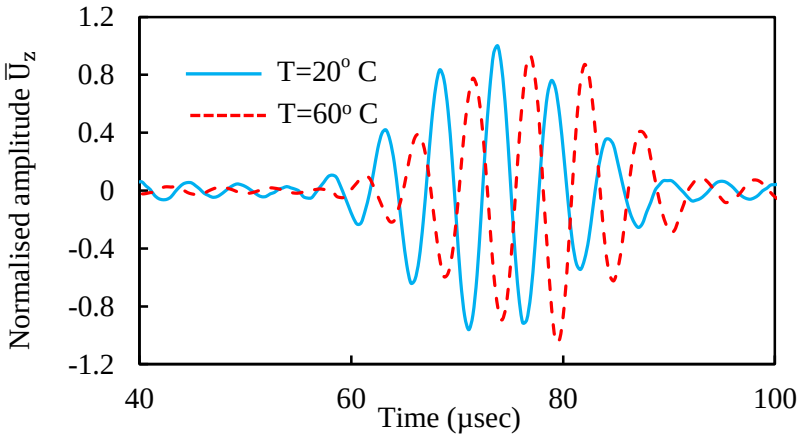

Figure 5: Normalised out-of-plane ($\bar{U}_z$) base-line time-traces at 20^oC and 60^oC as recorded with SLV for point P_1 at 200 kHz.

Other displacement components (U_x and U_y) had a much lower magnitudes as a result of the anti-symmetric mode, A_o, excitation, which largely involves the out-of-plane components of displacement and velocities. From figure 5 it is easy to note that the combined changes of material properties of the aluminium alloy, transducer and bonding due to the rise of the temperature have led to a lower group velocity and stretching of the time-trace. These effects are in agreement with the previous studies mentioned in the Introduction. All components of the velocity field over the scanning area were averaged, filtered and recorded for the use in the numerical reconstruction of the base-line time-trace to be described next.

Our previous preliminary experimental and numerical investigations on the influence of different parameters of the proposed method (such as grid measurement density, width of the scanning area, time-step in numerical investigations, signal filtering, etc.) on the error of the numerical reconstruction of the base-line time-trace have been described elsewhere (e.g. [37]). These extensive investigations provided us with the set of parameters, which was a compromise between the required accuracy and complexity of the modelling. Thus, the main purpose of the results presented below is to demonstrate the feasibility of the proposed method for the reconstruction of the base-line time-trace and damage detection under changing EOC.

For the reconstruction of the base-line time-trace a 3D Finite Element model representing an isotropic homogeneous plate with the dimensions with the same dimensions as in the experimental study with a circular dummy area in the middle of the plate was developed using the ANSYS 15.0 software package. The FE model utilised 3D hexahedral type of element with hourglass control with a characteristic size of 0.5 mm × 0.5 mm × 0.5 mm. The mesh density was roughly 20 nodes per wavelength or six elements across the thickness, which exceeds the minimum required number of nodes per wavelength reported in the literature [18, 38]. Each node of the hex element had three displacement degrees of freedoms. The finite element mesh was constructed to align the measurement grid with the corresponding surface nodes of FE mesh.

The boundary-value transient problem was analysed with the AutoDyne solver. The elastic properties were extracted from the dispersion equation (1) for both temperatures (20^{o}C and 60^{o}C). Poisson's ratio was set 0.3. The time step was automatically controlled by ANSYS/AutoDyne. A typical snap-short of transient displacement field is shown in figure 6. More details of the numerical approach adopted for the reconstruction of the base-line time-trace can be found in [37].

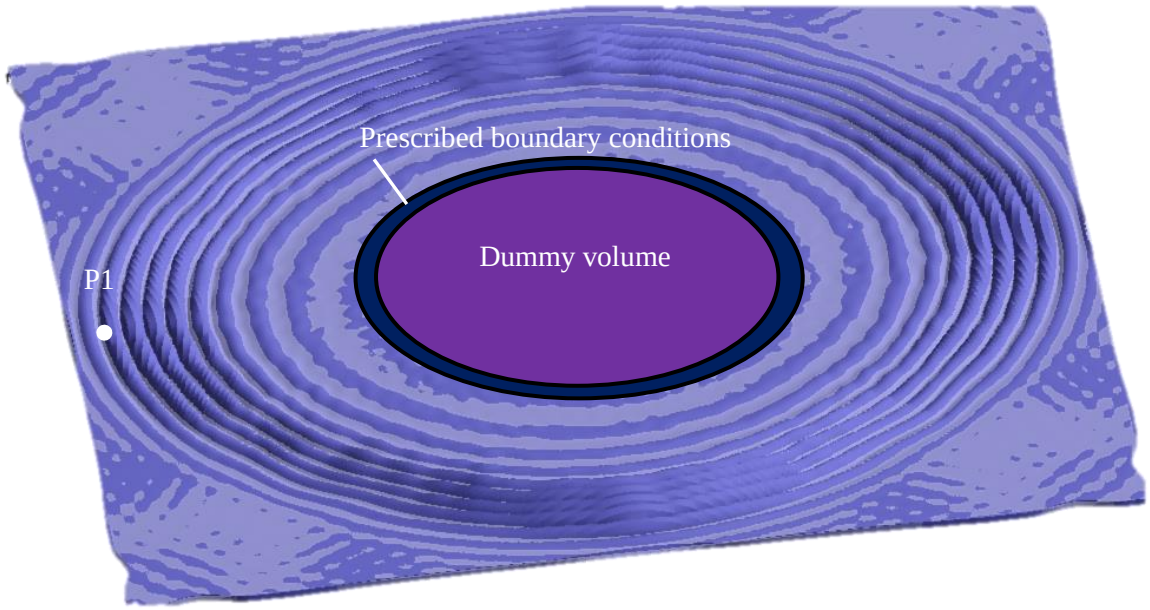

Figure 6: Typical snap-shot of FE simulations showing the dummy volume and prescribed boundary condition area for the aluminium plate and *f*=200 kHz centre frequency.

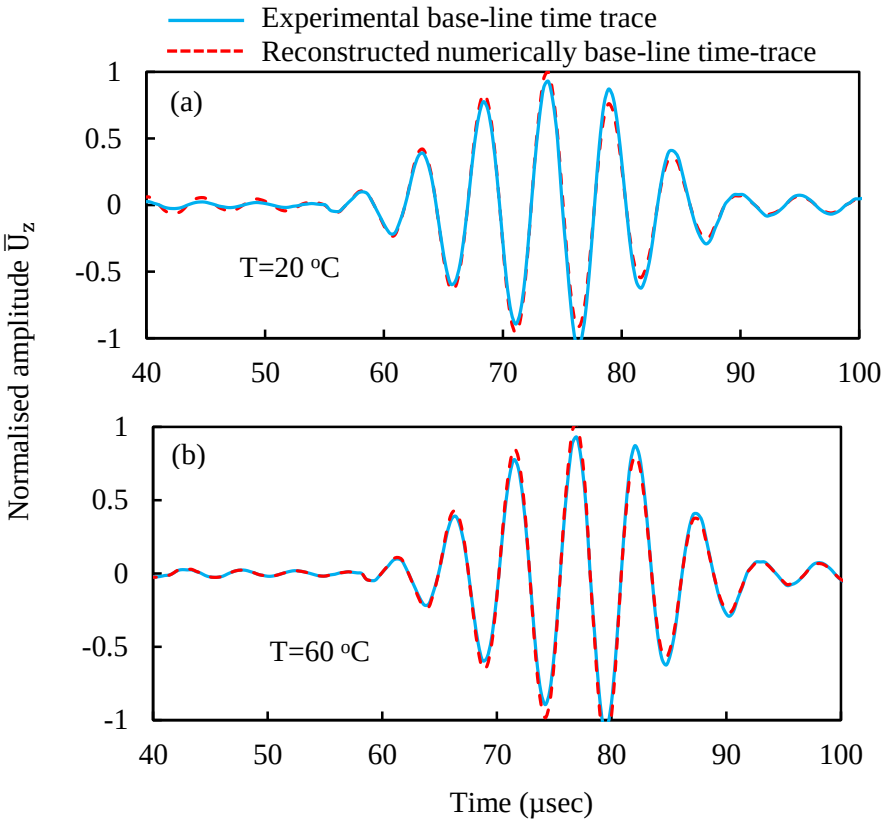

Figure 7: Comparison of the normalised out-of-plane base-line time-traces as obtained from the experiments (solid line) and numerical simulations (dotted line) for two temperatures (20 ^{o}C and 60 ^{o}C) and f = 200 kHz.

4. Results and Discussion

Figure 7 (a) and (b) show a comparison of the base-line time-traces as obtained from the experimental studies and numerical simulations, respectively, at two considered temperatures for the central frequency of the tone-burst of 200 kHz. A very good agreement can be observed, specifically for the shape of the signal. Small discrepancies between the experimental and numerically reconstructed traces were attributed to unavoidable simplifications and assumptions associated with the development of any FE model as well as with numerical errors due to finite discretisation.

Figure 8 shows a comparison of the error associated with the numerical reconstruction of the base-line time-trace (solid line) and substruction of two base-line time-traces at different temperatures. This comparison clearly indicates that the disregard of changing temperature can easily mask damage. The subtraction of two base-line signals at different temperatures has resulted in a residual time-trace with larger amplitude than the amplitudes of base-line time-traces. In addition, this figure confirms that with the proposed method the relative error of the numerical reconstruction of the time-traces is quite small, which allows applying this method for damage detection. In practical damage detection this error can be linked to the threshold level of the residual time-trace, which indicates the presence of a critical damage.

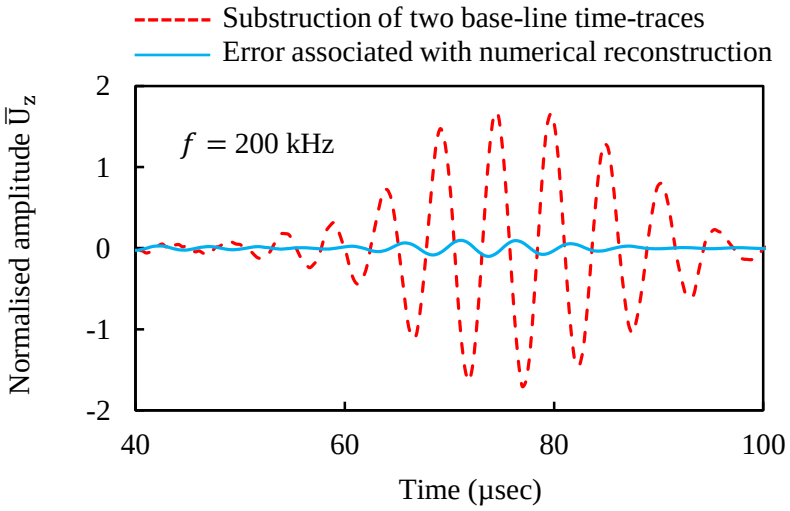

Figure 8: Error associated with the numerical reconstruction of the base-line time-trace (solid line) and substruction of two base-line time-traces at different temperatures, 20°C and 60°C (dotted line).

3.4 Damage Detection

This section details an application of the developed method for the detection of damage. Figure 4 illustrates a schematic diagram of a simple SHM system arranged in a pitch-catch mode. A cylindrical blind hole with a radius of 5 mm and depth 1.5 mm representing damage is located at a distance of 75 mm from the PZT. Figure 9 shows a time-trace at point, P_2, which is affected by the presence of the damage (dotted line). This time trace was recorded by SLV. In the same figure we show the base-line time-trace reconstructed numerically in accordance with the proposed method. One can clearly see the difference in time-traces, primary in the shape of the signals.

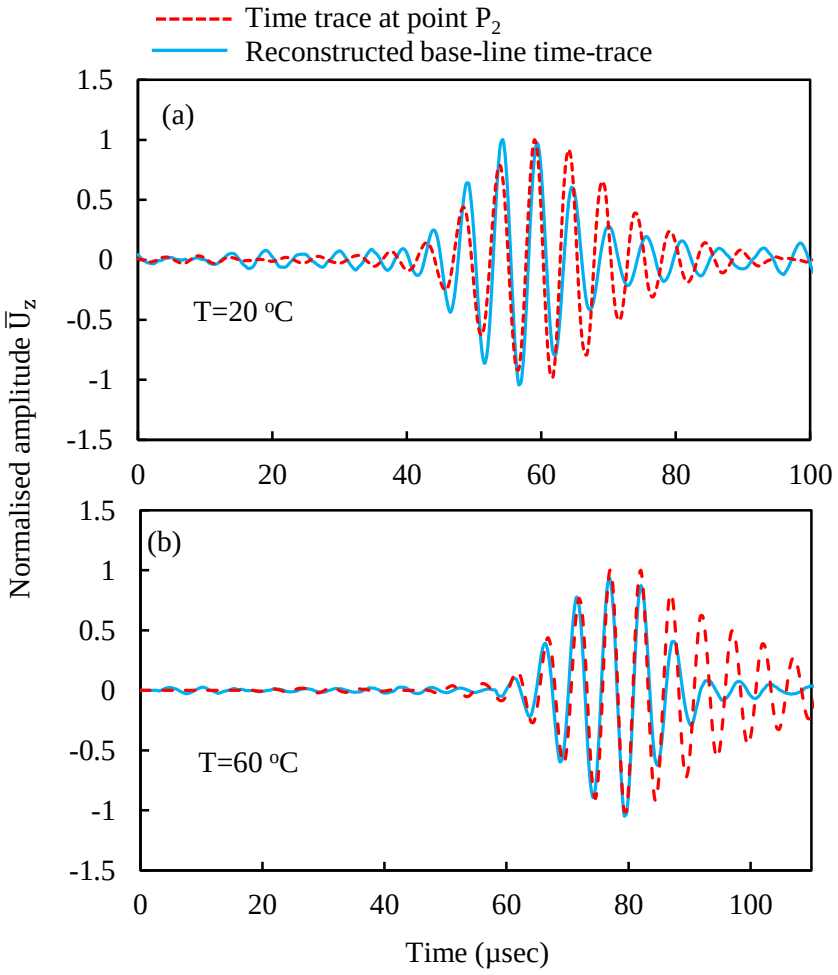

Figure 9: Measured time-trace and reconstructed numerically base-line time trace at the same point: f =200 kHz and temperature 20°C and 60 °C.

The substruction of two time-traces (damage signature or residual time-trace) is shown in figure 10 together with the typical error associated with the numerical reconstruction of the base-line time-trace. It can be seen from this figure that the magnitude of the signal associated with the numerical error is significantly less than the residual time-trace. This demonstrates that the considered damage can be reliably detected with the current method, and this method does not need any additional compensation for changing temperature conditions. The obtained results also suggest that the governing parameters of the method have been selected appropriately and there is no need for further refinement of FE or measurement mesh in order to improve the accuracy of the base-line time-trace reconstruction. As mentioned before, we omitted the outcomes of the extensive preliminary studies, based on which these governing parameters were selected.

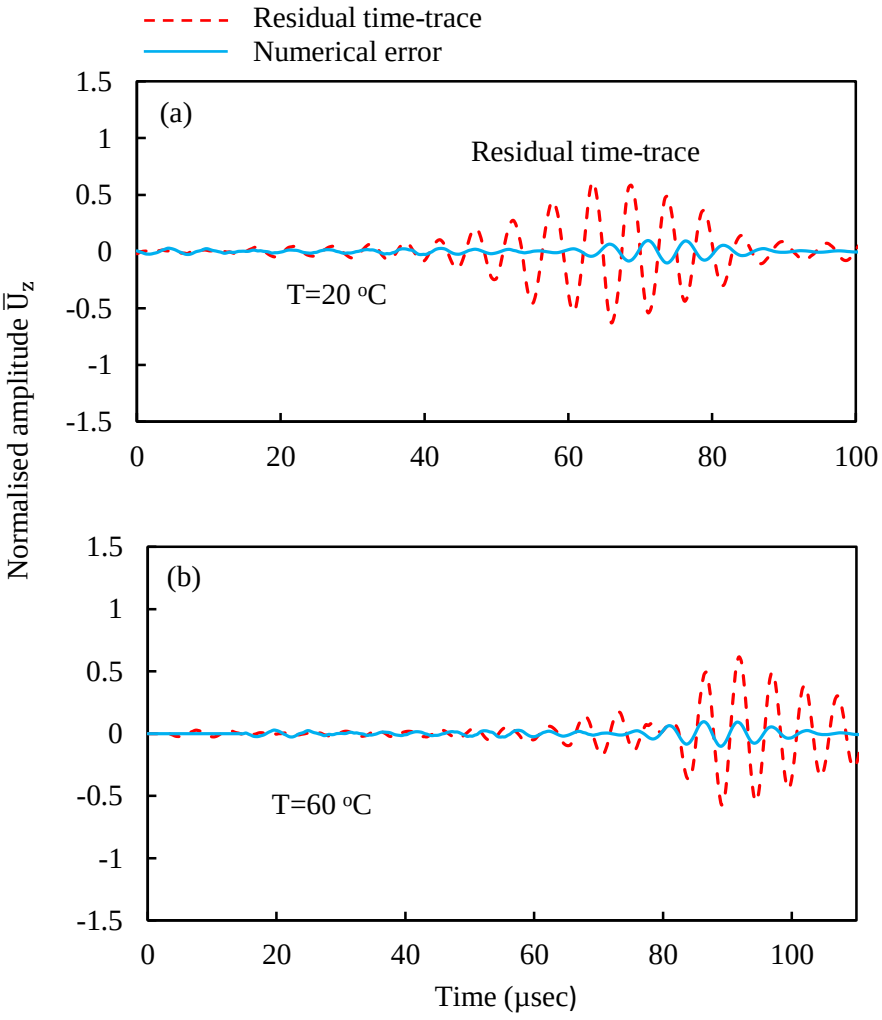

Figure 10: Residual time-trace and numerical error in reconstruction of base-line time-trace: f =200 kHz and temperature 20 °C and 60 °C.

4. Conclusions

A new method to compensate the effects of temperature variation on guided wave-based damage detection was presented in this paper. The proposed method is based on the application of 3D scanning laser vibrometry measurements in conjunction with explicit high-fidelity FE simulations of guided wave propagation in a free-from-defects structure. This method can help to overcome the current difficulties associated with the necessity to compensate for the uncontrolled factors affecting the base-line signal, such as temperature or humidity variations or material degradation. In this paper, in particular, it was demonstrated that the base-line signal can be reconstructed based on the measurements of the 3D velocity/displacement points near the PZT and prescribing these fields to the 3D transient FE model, which represent a free from defects structure.

In a general case, the accuracy of the reconstructed base-line time-trace, or, essentially the complexity of the FE model, density of the measurement points and the accuracy of the measurements, has to be selected based on the magnitude of the residual time-trace threshold accepted as the indication of damage in accordance with the common substruction approach. The time residual magnitude depends on the particular application of SHM and type of damage as discussed above. Therefore, the selection of the parameters, such as time step in numerical simulation, density of the measurement points and FE mesh, requires extensive preliminary numerical simulations as well as experimental studies in order to verify that the accuracy of the reconstructed base-line time trace is sufficient to detect the critical damage. However, once, the accuracy is verified then the method can be routinely applied to the similar structures working under changing EOC. Apart from many other techniques developed in the past the current method is capable to compensate the variation of several EOC, which can be of very different nature.

The method avoids the need to model the PZT response, which can be affected by various EOC. Another important aspect of the method is that the accuracy of the generation of the reconstructed base-line time-trace can be controlled by selecting the appropriate mesh and measurement grip density and time step. It was confirmed by direct experiments that the method is capable of taking into account EOC, specifically, temperature variation (which is the focus of the current paper) as well as the changes in material properties. The paper also described a practical implementation of the new method to damage detection at various temperatures, which demonstrates its feasibility.

It is recognised that the utilisation of 3D measurement system and transient FE simulations can significantly increase the cost of the damage detection. However, it is believed, that with the advance of computer and laser technologies the cost-efficiency can be significantly improved, and, in the future, the method can find a wide application in many industries and applications. Currently, this method can be used for damage detection in hard-to-reach locations or for periodical updated of base-line time-traces in the cases of changing EOC.

The future work will be primary directed to more complicated structures and composite components, where guided wave based defect detection techniques are considered to be a very promising for the development of on-line health monitoring systems. However, in the case of composite structures, the required size of the scanning area may be significantly larger as a result of a much more complicated wave structure generated by actuator (PZT) and the necessity to identify more material constants for accurate reconstruction of the base-line time-trace.

Acknowledgement

This work was supported by the Australian Research Council (ARC) under Grant Number DE130100261.

References

1. Wildy S J, Kotousov A, Codrington J, A new passive defect detection technique based on the principle of strain compatibility. *Smart Materials and Structures* 2008 **17**(4) 045004-045012.
2. Raghavan A, Cesnik C E S, Review of guided-wave structural health monitoring. *Shock and Vibration Digest* 2007 **39**(2) 91-116.
3. Giurgiutiu V, Structural health monitoring with piezoelectric wafer active sensors 2008 *Academic Pr*.
4. Giurgiutiu V, Zagrai A, Bao J J, Piezoelectric wafer embedded active sensors for aging aircraft structural health monitoring. *Structural Health Monitoring* 2002 **1**(1) 41-61.
5. Su Z, Ye L, Identification of damage using Lamb waves: from fundamentals to applications. *Springer Science & Business Media* 2009 Volume **48**.
6. Tian Z, Leckey C, Rogge M, Yu L, Crack detection with Lamb wave wavenumber analysis. *SPIE Smart Structures and Materials+ Nondestructive Evaluation and Health Monitoring International Society for Optics and Photonics* 2013.
7. Bai L, Yun Tian G, Simm A, Tian Sh, Cheng Y, Fast crack profile reconstruction using pulsed eddy current signals. *NDT & E International* 2013. **54**: 37-44.
8. Le Clézio E, Castaings M, Hosten B, The interaction of the S-0 Lamb mode with vertical cracks in an aluminium plate. *Ultrasonics* 2002. **40**(1) 187-192.
9. Rajagopal P, Lowe M J S, Scattering of the fundamental shear horizontal guided wave by a part-thickness crack in an isotropic plate. *The Journal of the Acoustical Society of America* 2008. **124** 2895-2904.
10. Sohn H, Park G, Wait J R, Limback N P, Farrar C R, Wavelet-based active sensing for delamination detection in composite structures. *Smart Materials and Structures* 2004. **13**: 153-160.
11. Su Z, Ye L, Lamb wave-based quantitative identification of delamination in CF/EP composite structures using artificial neural algorithm. *Composite structures* 2004. **66**(1–4) 627-637.
12. Sohn H, Swenson E D, Olson S E, DeSimio M, Dutta P, Debaditya Delamination detection in composite structures using laser vibrometer measurement of lamb waves. *SPIE Smart Structures and Materials+ Nondestructive Evaluation and Health Monitoring International Society for Optics and Photonics*2010.
13. Sohn, H., Dutta D, Yang J Y, DeSimio M, Olson S, Swenson E, Automated detection of delamination and disbond from wavefield images obtained using a scanning laser vibrometer. *Smart Materials and Structures* 2011. **20** 045017-045027.
14. Hosseini S, Lakis A A, Application of time–frequency analysis for automatic hidden corrosion detection in a multilayer aluminum structure using pulsed eddy current. *NDT & E International* 2012. **47** 70-79.
15. Sharma S, Mukherjee A, Ultrasonic guided waves for monitoring corrosion in submerged plates. *Structural Control and Health Monitoring* 2015. **22**(1) 19-35.
16. Pei J, Yousuf M I, Degertekin F L, Honein B V, Khuri-Yakub B T, Lamb wave tomography and its application in pipe erosion/corrosion monitoring. *Research in Nondestructive Evaluation* 1996. **8**(4) 189-197.
17. Ng C T, Veidt M, Scattering of the fundamental anti-symmetric Lamb wave at delaminations in composite laminates. *The Journal of the Acoustical Society of America* 2011. **129** 1288-1296.
18. Ng C T, Veidt M, A Lamb-wave-based technique for damage detection in composite laminates. *Smart Materials and Structures* 2009. **18**(7) 074006-074018.
19. Konstantinidis G, Drinkwater B W, Wilcox P D, The temperature stability of guided wave structural health monitoring systems. *Smart Materials and Structures* 2006. **15** 967-976.
20. Sohn H, Effects of environmental and operational variability on structural health monitoring. *Philosophical Transactions of the Royal Society of London A: Mathematical, Physical and Engineering Sciences* 2007. **365**(1851) 539-560.
21. Lee B, Manson G, Staszewski W, Environmental effects on Lamb wave responses from piezoceramic sensors. *Materials Science Forum Trans Tech Publ* 2003.
22. Ambroziński Ł, Magda P, Stepinski T, Uhl T, Dragan K, A method for compensation of the temperature effect disturbing Lamb waves propagation. *40th annual review of progress in*

quantitative nondestructive evaluation: *Incorporating the 10th International Conference on Barkhausen Noise and Micromagnetic Testing* 2014 *AIP Publishing.*
23. di Scalea F L, Salamone S, Temperature effects in ultrasonic Lamb wave structural health monitoring systems. *The Journal of the Acoustical Society of America* 2008. **124**(1) 161-174.
24. Putkis O, Dalton R P, Croxford A J, The influence of temperature variations on ultrasonic guided waves in anisotropic CFRP plates. *Ultrasonics* 2015. **60** 109-116.
25. Ha S, Lonkar K, Mittal A, Chang F K, Adhesive layer effects on PZT-induced lamb waves at elevated temperatures. *Structural Health Monitoring* 2010. **9**(3) 247-256.
26. Wilcox, P, Croxford AJ, Michaels JE, Lu Y, Drinkwater BW, A comparison of temperature compensation methods for guided wave structural health monitoring. *Review of progress in quantitative nondestructive evaluation: 34th Annual Review of Progress in Quantitative Nondestructive Evaluation* 2008. *AIP Publishing*.
27. Wang Y, Gao L, Yuan S, Qiu L, Qing X, An adaptive filter–based temperature compensation technique for structural health monitoring. *Journal of Intelligent Material Systems and Structures* 2014. **25**(17) 2187-2198.
28. Dan C A, Kudela P, Ostachowicz W, Compensation of Temperature Effects on Guided Wave Based Structural Health Monitoring Systems. *EWSHM-7th European Workshop on Structural Health Monitoring* 2014.
29. Croxford A J, Moll J, Wilcox P D, Michaels J E, Efficient temperature compensation strategies for guided wave structural health monitoring. *Ultrasonics* 2010. **50**(4–5) 517-528.
30. Rose J L, Ultrasonic Waves in Solid Media 2014 New york: *Cambridge University Press*.
31. Ong W H , Rosalie C, Rajic N, Chiu W K, Determination of Elastic Properties in a Plate by Lamb Wave Analysis and Particle Swarm Optimisation. *Procedia Engineering* 2014. **75**(0) 39-44.
32. Hayashi Y, Ogawa S, Cho H, Takemoto M, Non-contact estimation of thickness and elastic properties of metallic foils by laser-generated Lamb waves. *NDT & E International* 1999. **32**(1) 21-27.
33. Eremin, A A, Glushkov E V, Glushkova N V, Lammering R, Evaluation of effective elastic properties of layered composite fiber-reinforced plastic plates by piezoelectrically induced guided waves and laser Doppler vibrometry. *Composite Structures* 2015. **125** 449-458.
34. Ambrozinski L, Packo P, Pieczonka L, Stepinski T, Uhl T, Staszewski W J. Identification of material properties–efficient modelling approach based on guided wave propagation and spatial multiple signal classification. *Structural Control and Health Monitoring* 2015. **22**(7) 969-983.
35. Spencer A B, Worden K, Staszewski W J, Rongong J A, Sims N D. An Optimisation Scheme Based on the Local Interaction Simulation Approach and Lamb Waves for Elastic Property Estimation in Multi-Layered Composites. *Shock and Vibration* 2012. 19(5) 1027-1040.
36. Weisbecker, H., Cazzolato B, Wildy S, Marburg S, Codrington J, Kotousov A, Surface strain measurements using a 3D scanning laser vibrometer. *Experimental mechanics* 2012. **52**(7) 805-815.
37. Aryan P, Kotousov A, Ng, C T, Cazzolato B S, An approach towards a baseline-free technique for damage detection utilising advances in 3D laser vibrometry. *8th Australasian Congress on Applied Mechanics* 2014. *Melbourne*.
38. Lowe M J S, Cawley P, Kao J Y, Diligent O, The low frequency reflection characteristics of the fundamental antisymmetric Lamb wave a from a rectangular notch in a plate. *The Journal of the Acoustical Society of America* 2002. **112**(6) 2612-2622.